Optics Communications 356 (2015) 411–415

Contents lists available at ScienceDirect

Optics Communications

journal homepage: www.elsevier.com/locate/optcom

High-order Stokes generation in a KTP Raman laser pumped by a passively Q-switched ND:YLF laser

Maorong Wang [a,b], Kai Zhong [a,b,*], Jialin Mei [a,b], Shibei Guo [a,b], Degang Xu [a,b], Jianquan Yao [a,b]

[a] School of Precision Instrument and Opto-electronics Engineering, Institute of Laser and Opto-Electronics, Tianjin University, Tianjin 300072, China
[b] Key Laboratory of Opto-electronics Information Technology, Tianjin University, Ministry of Education, Tianjin 300072, China

ARTICLE INFO

Article history:
Received 14 July 2015
Received in revised form
5 August 2015
Accepted 11 August 2015

Keywords:
Raman laser
KTP
Nd:YLF
Passively Q-switched

ABSTRACT

High-order Stokes wave was observed in an x-cut KTP crystal based on stimulated Raman scattering (SRS) pumped by a passively Q-switched Nd:YLF laser with a Cr^{4+}:YAG saturable absorber. Output spectra including the fundamental wave at 1047 nm and six Stokes wavelengths at 1077 nm, 1110 nm, 1130 nm, 1143 nm, 1164 nm, 1180 nm based on two Raman frequency shift at 267.4 cm^{-1} and 693.0 cm^{-1} were obtained simultaneously. We also detected green light generation with output power of 12 mW from self frequency mixing in the KTP crystal. The maximum total output power reached 452 mW at the repetition frequency of 8.1 kHz, corresponding to the optical-to-optical conversion efficiency of 4.61% and pump-to-Raman conversion efficiency of 3.6%.

1. Introduction

Raman lasers based on nonlinear stimulated Raman scattering (SRS) effect are very important in generating new spectral lines that is impossible for direct laser transition in gain medium. They also occupy an important position in coherent yellow–orange source through frequency doubling, which have wide applications in medical treatment, metrology, and remote sensing. The most popular Raman crystals are $LiIO_3$, $BaNO_3$, vanadates, tungstates, molybdates and so on. Some of them can also be used as laser gain materials by doping Nd^{3+} ions and compact self-Raman lasers can be achieved [1–5], while some of them have excellent properties of both SRS and second harmonic generation (SHG) for compact and efficient self-frequency-doubled laser in the visible range [6]. Recently, high-power self-Raman lasers and efficient self-frequency-doubled yellow lasers have been reported.

As one kind of the most famous and successful nonlinear crystals, the KTP family (KTP, KTA etc.) have good optical quality, high damage threshold, wide transmission and phase matching range, large nonlinearity, and large acceptance angle, possessing wide applications in SHG and optical parametric oscillators (OPOs) [7–9]. As one of the isomorphs, KTA has even broader transmission range in the mid-infrared [10]. Besides the second order nonlinearity, both KTP and KTA are also attractive third-order nonlinear materials for efficient Raman lasers. Watt-level Raman lasers have been reported [11–15]. Combining its ability in SHG, high-power self-frequency-doubled yellow laser have been realized [16]. As KTP and KTA have obvious Raman gain with small frequency shifts at 200–300 cm^{-1}, multi-wavelength Raman lasers containing high-order Stokes waves are also feasible with broadly coated cavity mirrors [11–15].

In this paper, we present high-order Stokes generation with a KTP crystal pumped by a passively Q-switched Nd:YLF laser at 1047 nm. Nd:YLF crystal is an uniaxial birefringent crystal that shows distinct emission characteristics between the σ polarization and π polarizations, and there are two alternative polarized wavelengths (1047 nm and 1053 nm) for flexible frequency conversion. The fluorescence lifetime of Nd:YLF is much longer than Nd:YAG and Nd:YVO_4 etc., which give it higher energy storage ability for Q-switching. Moreover, the dn/dT coefficient of Nd:YLF is negative, greatly decreasing the thermal lensing effects. Compared with actively Q-switching, passively Q-switching is more compact and simple, needless of extra electrical drivers. In the experiment the higher-gain 1047 nm laser line was used as the fundamental wavelength. Owing to the high-Q cavity, six Stokes lines including 4 orders at 1077.4 nm, 1109.7 nm, 1129.6 nm, 1143.4 nm, 1164.3 nm and 1180.1 nm were observed simultaneously, based on cascaded stimulated Raman scattering of two modes at 267.4 cm^{-1} and 693.0 cm^{-1}. We also obtained visible laser generation at 538.5 nm by frequency mixing of the infrared laser lines. While the incident diode pump power was 9.8 W, the total output power was

* Correspondence to: Institute of Laser and Optoelectronics, College of Precision Instrument and Optoelectronics Engineering, Tianjin University, Tianjin 300072, China. Fax: +86 22 27407676.
E-mail address: zhongkai1984@gmail.com (K. Zhong).

http://dx.doi.org/10.1016/j.optcom.2015.08.031
0030-4018/

464 mW, including 102 mW fundamental laser power, 350 mW Stokes power and 12 mW green laser power. The pulse train of the multi-wavelength KTP Raman laser was observed, revealing the dynamic process of Stokes cascading. Each of the pulses had a pulse width of around 20 ns at the maximum output power and the corresponding repetition rate was 8.1 kHz. As far as we know, this was the largest Stokes line number generated by KTP/KTA Raman lasers.

2. Experimental setup

The experimental setup of the multi-wavelength KTP Raman laser is shown in Fig. 1. The pump source was a 50-watt 808 nm laser diode coupled by fiber with the core diameter of 400 μm and numerical aperture of 0.22. It was focused into the Nd:YLF laser crystal by coupling system at a spot size of 320 μm. The gain medium was an a-cut Nd:YLF crystal with the size of 3 mm × 3 mm × 10 mm and doping concentration of 1 at%. It was anti-reflection (AR) coated at pump wavelength ($R<2\%$@808 nm) and resonant fundamental wavelength ($R<0.2\%$@1040–1060 nm). The nonlinear crystal was an x-cut ($\theta=90°$, $\phi=0°$) KTP crystal with the size of $4\times4\times10$ mm^3, both faces AR coated at fundamental and Stokes wavelengths ($R<0.2\%$@1047 nm, $R<0.5\%$ @1100 nm). Both the Nd:YLF and KTP crystals were wrapped by indium foil and mounted in copper heat sinks. The heat generated in the Nd:YLF crystal was taken away by circulating water while the KTP temperature was stabilized by a thermal electric cooler (TEC). An AR ($R<0.2\%$) coated Cr:YAG crystal (⌀10 mm × 1.8 mm) with a small signal transmission of 93% was inserted between the two crystals and employed as a saturable absorber for passively Q-switching. The resonant cavity was in a linear plane-concave configuration. The input mirror (IM) was plano-concave with its both faces coated for high transmission (HT) at 808 nm ($T>98\%$) and the concave facet also coated for high reflection (HR) at 1047 nm ($R>99.8\%$). The output coupler (OC) was plane-parallel and coated for HR at fundamental wavelength ($R>99.8\%$) and partial transmission (PR) at Stokes wavelengths.

3. Experimental results and discussion

In order to achieve efficient high-order Raman lasing in KTP with a lower threshold, the nonlinear crystal should be long enough to enhance Raman gain and the cavity loss for fundamental and low-order Raman wavelengths should be minimized to keep higher intracavity intensity [15]. The detailed transmissions of the output couplers used in the experiment at several special Stokes wavelengths from 1.06 μm to 1.2 μm is listed in Table 1. Low transmission output couplers are utilized for high-order Stokes generation in high-Q resonant cavities. The long upper level lifetime of the Nd:YLF laser crystal yields excellent energy storage ability, which is also good for decreasing the pumping threshold with large pulse energy and high peak power fundamental laser.

It was found that the threshold pump power was about 2 W using all the three output couplers, around which only one Stokes wavelength was generated with a polarization state vertical to the fundamental wave. With the increase of pump power, several Stokes orders emerged almost simultaneously with all the three different output couplers, and their relative intensities kept rising proportionally. Detected with an Agilent 86142B optical spectrum analyzer, six stable Stokes wavelengths besides the fundamental wavelength were found, shown in Fig. 2(a)–(c). Their wavelengths were 1077.4 nm, 1109.7 nm, 1129.6 nm, 1143.4 nm, 1164.3 nm, and 1180.1 nm respectively. According to Ref. [17], the two strongest Raman peaks located at 267.4 cm^{-1} and 693.0 cm^{-1}. It was easy to know that Stokes wavelength at 1077.4 nm, 1109.7 nm, 1143.4 nm and 1180.1 nm came from the first, second, third and fourth order SRS of the 267.4 cm^{-1} mode based on the fundamental wavelength at 1047.6 nm. The Stokes wavelength at 1129.6 nm was the first order SRS of the 693 cm^{-1} mode, and 1164.3 nm was the cascaded SRS of the 267.4 cm^{-1} and 693.0 cm^{-1} modes.

Although it was hard to distinguish every Stokes wavelength and measure their output characteristics individually, we were able to separate the fundamental wave from all the output Stokes wavelengths with a filter that was HR ($R>95\%$) below 1060 nm and HT ($R<2\%$) between 1070 nm and 1200 nm. Measured with a Physcience LP-3A power meter, the relationship between the incident diode laser power and total Stokes power is shown in Fig. 3. The maximum Stokes power was 350 mW pumped at 9.8 W while M1 is used as the output coupler, corresponding to the pump-to-Stokes conversion of 3.56%. The laser power reflected by the filter was 102 mW, thus the total output power is 452 mW and the diode-to-infrared conversion efficiency was 4.61%. The maximum total output powers using the other two output couplers were 392 mW and 235 mW, and their conversion efficiencies were 4% and 2.4%. There were several reasons restricting the output power enhancement, like leakage of Stokes through the input mirror, unsatisfying AR coatings above 1100 nm for Nd:YLF, Cr:YAG and KTP crystals and so on. Estimating from the relative intensities in the output spectra, the maximum powers obtained with M1 at 1077.4 nm, 1109.7 nm, 1129.6 nm, 1143.4 nm, 1164.3 nm, and 1180.1 nm should be around 46 mW, 53 mW, 83 mW, 132 mW, 24 mW, 13 mW, respectively.

Detected by a fast-response InGaAs photodiode (Thorlabs DET08C) and recorded by a Tektronix TDS620B oscilloscope, the temporal pulse shape of the free-running fundamental wave (without nonlinear crystal), depleted fundamental wave, and Stokes wave are shown in Fig. 4. Significant depletion could be concluded from Fig. 4(a) and (b), where a sharp decrease emerged

Table 1
Output mirror reflectivity at different Stokes lines.

OC	Wavelength					
	1077 nm	1110 nm	1130 nm	1143 nm	1164 nm	1180 nm
M1	0.99727	0.99443	0.98906	0.98815	0.98625	0.97721
M2	0.99521	0.99705	0.99690	0.99598	0.99116	0.97631
M3	0.99880	0.99854	0.99751	0.9959	0.98803	0.96732

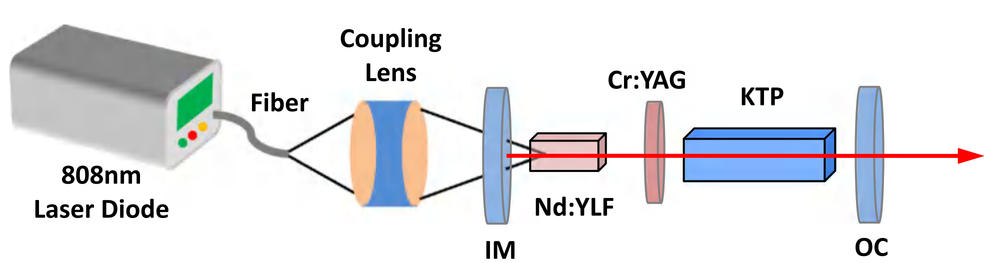

Fig. 1. Experimental setup of the multi-wavelength KTP Raman laser.

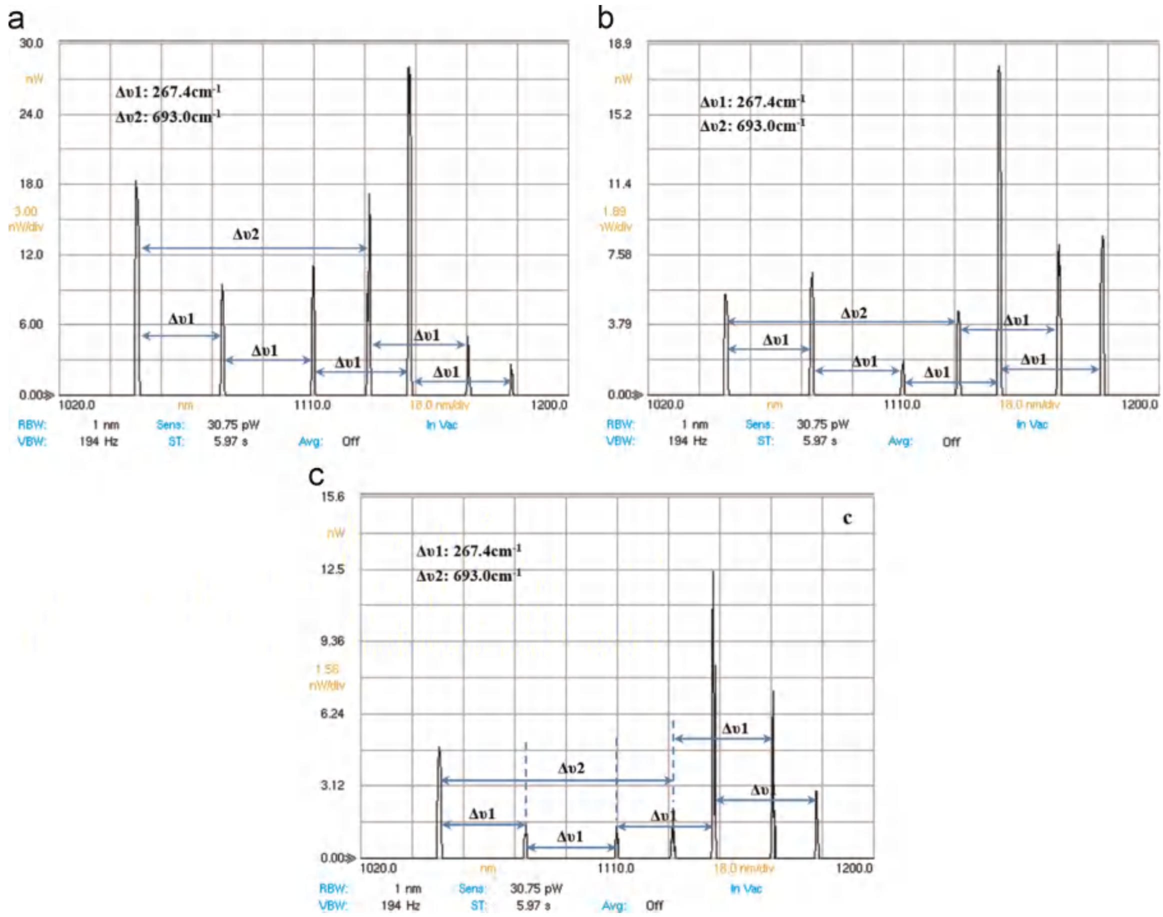

Fig. 2. Output spectra of the KTP Raman laser with different output couplers M1 (a), M2 (b) and M3 (c).

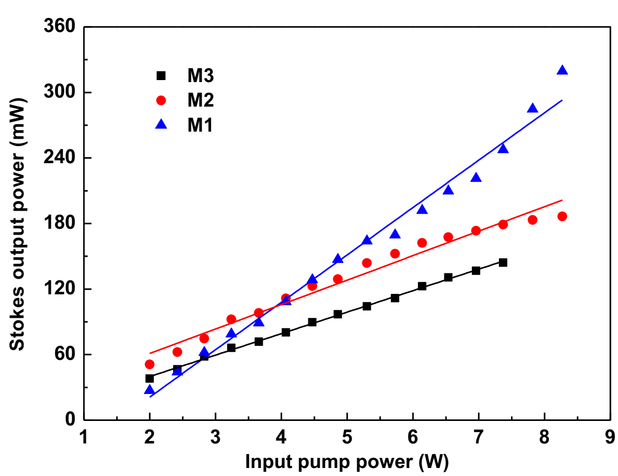

Fig. 3. Stokes wave output power versus input pumped power with different output couplers.

in the fundamental pulse waveform when the pump intensity exceeded threshold. In Fig. 4(c), as the total pulse width containing the whole pulse train was much wider than that of a free-running fundamental wave, it could be concluded that depicted the temporal pulse shapes of the fundamental wave and Stokes waves at different orders. Four sub-pulses was generated during one pumping process, which was coincident with the maximum Stokes order of four. This was different from the experimental results obtained by the other researchers reported before. It could also be observed in Fig. 4(c) that the time delay between adjacent Stokes orders was about 120 ns. The pulse repetition rate varied from 1.4 kHz to 8.1 kHz when the diode pump was increased from near threshold to 9.8 W, shown in Fig. 5. Considering the pulse width was about 17 ns, the single pulse energy and peak power (in total) were about 3.28 kW and 55.8 μJ at maximum output power, respectively.

Bright visible laser in the green–yellow range could also be observed during the experiment. Using an Ocean Optics USB-4000 spectrometer (360–825 nm) and a short-pass filter, the visible spectra were recorded and shown in Fig. 6. When the pump power was around threshold, four visible lines at 523.5 nm, 538.5 nm, 546.8 nm, and 555 nm were detected, in which the 538.5 nm line was much stronger than the other three. Slightly increasing diode pump power, only the 538.5 nm laser line existed while the other laser lines were too weak to be picked out. Considering there were many factors affecting the efficiency of frequency mixing, such as phase-matching (PM), laser intensity, polarization, etc., we could not determine whether the 538.5 nm laser line came from frequency doubling of 1077 nm or sum frequency mixing of 1047 nm and 1110 nm, both of which were far from perfect PM conditions. The maximum green laser power at 538.5 nm was 12 mW.

4. Conclusion

In conclusion, a multi-wavelength laser is demonstrated based on a passively Q-switched 1047 nm Nd:YLF laser pumped KTP Raman laser. Six Stokes lines covering the wavelength range from 1077 nm to 1080 nm with the highest order of 4 was obtained. Pump at 9.8 W, the maximum output power was 452 mW,

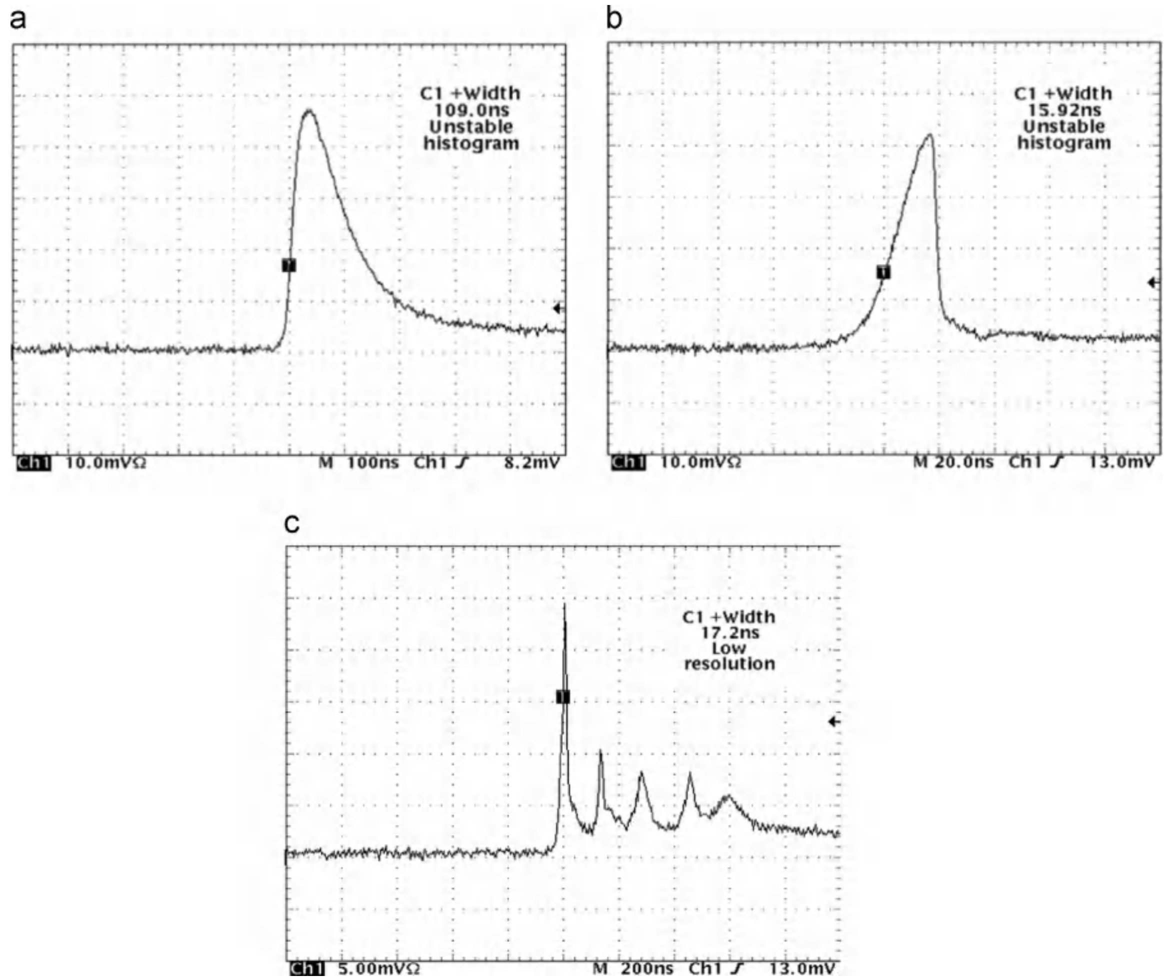

Fig. 4. Temporal pulse shapes of the free-running fundamental wave (a), depleted fundamental wave (b) and Stokes waves (c).

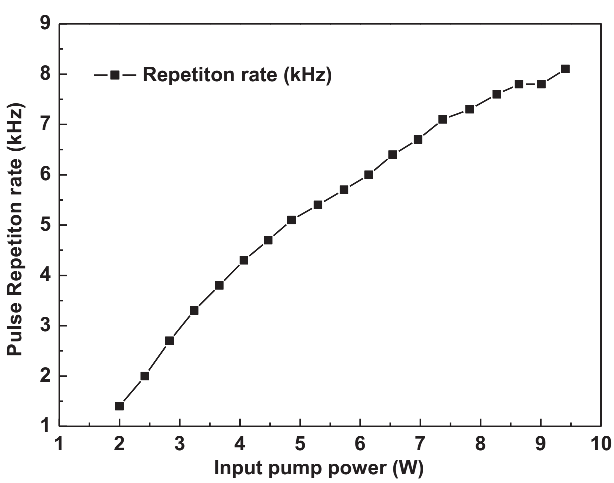

Fig. 5. Repetition rate versus input pump power.

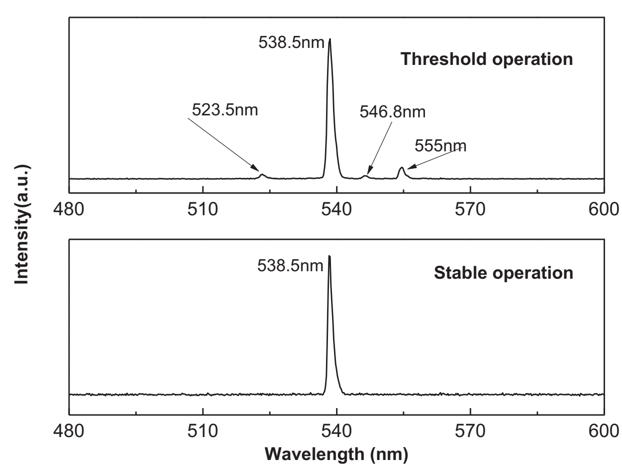

Fig. 6. Visible laser spectra generated from frequency mixing in KTP crystal.

including Stokes power of 350 mW, fundamental laser power of 90 mW and green laser power of 12 mW, corresponding to the total optical-to-optical conversion efficiency of 4.61% and Stokes conversion efficiency of 3.6%. The temporal pulse shapes for fundamental and different Stokes lines were obtained, from which obvious fundamental depletion was observed and the energy transferring among different Stokes waves could be deduced, which could be further verified by a theoretical model for passively Q-switched Raman lasers in our future work. From the visible spectra, the frequency mixing process of fundamental and Stokes lines for visible lasers was also analyzed.

Acknowledgments

This work is supported by the National Basic Research Program of China (Grant no. 2014CB339802), National Natural Science Foundation of China (NSFC) (Grant nos. 61101058, 61172010 and

61471257), Tianjin Municipal Primary Application and Frontier Technology Research Plan (13JCQNJC01500), and Open foundation of Key laboratory of Opto-electronic Information Technology, Ministry of Education (Tianjin University).

References

[1] C.Y. Lee, C.C. Chang, P.H. Tuan, C.Y. Cho, K.F. Huang, Y.F. Chen, Opt. Lett. 40 (2015) 1996–1999.
[2] X. Ding, C. Fan, Q. Sheng, B. Li, X.Y. Yu, G.Z. Zhang, B. Sun, L. Wu, H.Y. Zhang, J. Liu, P.B. Jiang, W. Zhang, C. Zhao, J.Q. Yao, Opt. Express 22 (2014) 29121–29126.
[3] Z.C. Wang, C.L. Du, S.C. Ruan, L. Zhang, Opt. Laser Technol. 42 (2010) 716–719.
[4] C.Y. Tang, W.Z. Zhuang, K.W. Su, Y.F. Chen, IEEE J. Sel. Top. Quantum Electron. 21 (2015) 1400206.
[5] A.A. Kaminskii, H. Rhee, H.J. Eichler, K. Ueda, K. Oka, H. Shibata, Appl. Phys. B 93 (2008) 865–872.
[6] Z.L. Gao, S.D. Liu, J.J. Zhang, S.J. Zhang, W.G. Zhang, J.L. He, X.T. Tao, Opt. Express 21 (2013) 7821–7826.
[7] J.F. Yang, B.T. Zhang, J.L. He, H.T. Huang, X.L. Dong, J.L. Xu, C.H. Zuo, S. Zhao, X. Q. Yang, G. Qiu, Z.K. Liu, Appl. Phys. B 98 (2010) 49–54.
[8] K. Zhong, Y.Y. Wang, D.G. Xu, Y.F. Geng, J.L. Wang, P. Wang, J.Q. Yao, Appl. Phys. B 97 (2009) 61–66.
[9] H.Y. Zhu, G. Zhang, H.B. Chen, C.H. Huang, Y. Wei, Y.M. Duan, Y.D. Huang, H. Y. Wang, G. Qiu, Opt. Express 17 (2009) 20669–20674.
[10] K. Zhong, J.Q. Yao, D.G. Xu, J.L. Wang, J.S. Li, P. Wang, Appl. Phys. B 100 (2010) 749–753.
[11] H.Y. Zhu, Z.H. Shao, H.Y. Wang, Y.M. Duan, J. Zhang, D.Y. Tang, A.A. Kaminskii, Opt. Express 22 (2014) 19662–19667.
[12] Y.T. Chang, Y.P. Huang, K.W. Su, Y.F. Chen, Opt. Express 16 (2008) 8286–8291.
[13] H.W. Chu, K.J. Yang, T. Li, S.Z. Zhao, Y.F. Li, D.C. Li, G.Q. Li, J. Zhao, W.C. Qiao, IEEE Photon. Technol. Lett. 26 (2014) 2369–2371.
[14] H.W. Chu, S.Z. Zhao, K.J. Yang, Y.F. Li, G.Q. Li, D.C. Li, J. Zhao, W.C. Qiao, T. Li, Opt. Express 39 (2014) 723–726.
[15] K. Zhong, J.S. Li, D.G. Xu, X. Ding, R. Zhou, W.Q. Wen, Z.Y. Li, X.Y. Xu, P. Wang, J. Q. Yao, Laser Phys. 20 (2010) 750–755.
[16] Z.J. Liu, Q.P. Wang, X.Y. Zhang, S.S. Zhang, J. Chang, S.Z. Fan, W.J. Sun, G.F. Jin, X. T. Tao, Y.X. Sun, S.J. Zhang, Z.J. Liu, Opt. Express 34 (2009) 2183–2185.
[17] C.S. Tu, A.R. Guo, R.W. Tao, R.S. Katiyar, R. Guo, A.S. Bhalla, J. Appl. Phys. 79 (1996) 3235–3240.